



Contents lists available at ScienceDirect

International Journal of Multiphase Flow

journal homepage: www.elsevier.com/locate/ijmulflow

Investigation of the particle-laden airflow generated by a pseudo-machining operation

Emmanuel Belut^{a,1}, Francis Bonthoux^b, Benoît Oesterlé^{a,*}, Jean-Raymond Fontaine^b, Abdelhamid Kheiri^a

^a LEMTA, Nancy-University, CNRS, ESSTIN, 2 rue Jean Lamour, 54519 Vandoeuvre-lès-Nancy, France

^b INRS, avenue de Bourgogne, B.P. 27, 54501 Vandoeuvre-lès-Nancy, France

ARTICLE INFO

Article history:

Received 3 October 2008

Received in revised form 24 March 2009

Accepted 3 April 2009

Available online 12 April 2009

Keywords:

Lagrangian tracking

LES

Machining operation

Particle dispersion

PDPA

PIV

ABSTRACT

A test rig recreating a typical machining induced gas–solid flow is used to investigate the behaviour of the emitted pollutant particles and their effect upon the airflow around the machine tool. The flow is driven by a rotating cylinder and a tangential jet of inertial solid particles. Experimental data concerning both particle flow and air flow are collected by means of phase Doppler particle analyser (PDPA) and particle image velocimetry (PIV). After describing the specific treatments used to discriminate the two phases, complete results are provided and discussed. Additionally, with the main objective being to optimize the design of pollutant capture devices for machining systems, tentative numerical simulations are carried out and compared to experimental data. For the one-phase case (air flow without particles), good agreement between simulations and experiments is found and the superiority of a wall-function based large eddy simulation (LES) over realizable $k-\varepsilon$ modelling is highlighted. For two-phase cases, combination of LES and Lagrangian tracking with two-way coupling leads to simulation results that are reasonably accurate considering the low degree of modelling and the empiricism involved. Particle-to-particle collisions, disregarded in simulations, appear to be a predominant phenomenon in the jet source region, thus partly explaining some discrepancies observed between simulations and experiments.

© 2009 Elsevier Ltd. All rights reserved.

1. Introduction

Machining, and in particular the hard-metal machining sector, is an important source of employee exposure to inhalable dust carrying a health risk, cobalt being one example. In this respect, INRS (Institut National de Recherche et de Sécurité) is currently involved in developing a method to design pollutant capture devices based on numerical simulation of the two-phase flows (gas/particles) produced by machining systems. The particles of pollutants emitted during machining can generally be divided into two main types: small particles with short response time, presenting a health hazard, that are transported passively by the airflow, and bigger particles, whose health impact is low, but that affect massively the airflow and its turbulence, and hence the dispersion of the small particles. The main issue being to predict numerically the dispersion of these small particles, there is a need for a modelling approach that can accurately predict both turbulent flows gener-

ated by rotating pieces and turbulent flows driven by inertial particles.

Most of machining operations involving human operators generate airflows with typical Reynolds number ranging from 10^4 to 10^5 (based on the radius and rotation speed of the revolving element). The transient nature of the machining process, the presence of protruding parts on the rotating element (chuck jaws, teeth), as well as the time evolving geometry, make the existence of a stationary mean flow questionable if not impossible, hence the necessity of using transient simulations. Machining induced airflows are characterized by strong streamlines curvature, rotor–stator interactions, and turbulence occasionally dominated by vortices shed behind protruding parts of rotating elements. These characteristics are known to be unfavourable to RANS modelling. Experiments on three-dimensional turbulent boundary layers (typically encountered against a circular saw) revealed significant misalignment of the Reynolds shear stress vector with respect to the mean velocity gradient vector (Littell and Eaton, 1994; Bradshaw and Terrell, 1969), thus invalidating the concept of scalar eddy viscosity. More recently, while considering the case of a simple rotor–stator flow, Andersson and Lygren (2006) showed numerically that this misalignment could keep up far beyond the buffer region. Therefore isotropic RANS eddy-viscosity models are likely to fail

* Corresponding author. Tel.: +33 383 685080; fax: +33 383 685085.

E-mail addresses: belut@imft.fr (E. Belut), francis.bonthoux@inrs.fr (F. Bonthoux), benoit.oesterle@esstin.uhp-nancy.fr (B. Oesterlé), jeanraymond.fontaine@inrs.fr (J.-R. Fontaine), abdelhamid.kheiri@esstin.uhp-nancy.fr (A. Kheiri).

¹ Present address: IMFT, allée du Professeur Camille Soula, 31400 Toulouse, France.

partially in rotor–stator flows, and efficient modelling of machining airflows would require, at least, the use of an unsteady RANS model fully taking Reynolds stresses into account. In terms of computational complexity, large eddy simulation (LES) appears to be a competitive alternative, provided that the mesh requirements remain reasonable. This can be achieved by coarsely resolving the LES in the near-wall region, which is the most demanding zone in terms of spatial discretization, and modelling the flow using a wall-function in this region. This introduces quite a lot of empiricism, but can be partly justified in flows in which near wall turbulence is not a main issue. We found, however, that such a wall-function based LES performs surprisingly well for the specific case of the smooth spinning disc, where wall turbulence is fundamental (Belut et al., 2005). Additional evaluation of the performances of such a LES applied to real-like machining conditions can be obtained from comparison with the measurements performed on a test rig that was realized and instrumented to serve as a reference case.

The experimental apparatus and measurement techniques are described in the next Section, then the paper goes on to present the numerical methods used to compute the motion of the gaseous and discrete phases in the test rig. In Section 4, experimental results are given and discussed for both the single-phase airflow and the two-phase cases, and comparison is proposed with the numerical predictions to evaluate the interest of the simulation technique.

2. Experimental facility and measurement techniques

The original experimental apparatus developed, sketched in Fig. 1, has been briefly presented formerly (Belut et al., 2006). It is made up of an aluminum cylinder (diameter 130 mm, length 150 mm) rotating inside a transparent parallelepiped-shaped enclosure (400 × 400 × 600 mm). A particle jet recreating the ventilation effects of a real pollutant is obtained thanks to a feeding system that continuously pushes spherical glass microbeads in a metallic nozzle against the rotating cylinder, whose surface has

been made rough in order to help evacuate the particles by friction. The obtained particle jet is stable, and its flow rate is controlled.

2.1. Discrete phase measurements

Particle velocities, diameters, fluxes and concentration in the jet were measured using a phase Doppler particle analyser [PDPA] (Bachalo, 1994), thanks to a Dantec two components PDPA measurement system linked to a Dantec 50 N 10 PDA signal processing unit. The laser source employed was an Argon-Ion Coherent Innova 70-3 laser, the useful wavelengths being 514.5 and 488 nm. Measurements were taken in reflected light, the transmission and reception axes forming an angle of 100° (reflection angle of 80°). Samples of the glass particles employed were characterized beforehand with a Malvern Mastersizer granulometer in order to corroborate the results obtained by PDPA. This operation was repeated regularly during the measurement campaign, as the microbeads were recycled after use, which could have led to granulometric modifications given the abrasion to which particles were subjected in the feeding system. The particle sphericity was also checked in several samples with an optical microscope, as this criterion has a determining impact on the reliability of the granulometric measurements obtained by phase Doppler anemometry. An amount of irregularly shaped particles lower than 3% was certified by the producer, and observations showed that most of sphericity aberrations were in fact particles stuck together by the manufacturing process. The resulting bond between particles appeared to be easily broken during the transit of the particles in the feeding system. All these examinations revealed no significant microbead modification during use.

Two classes of particles were used in the study, namely 50–150 μm and 100–200 μm glass spheres. The diameter distributions can be efficiently modelled by a Rosin–Rammler law with parameters reported in Table 1.

As the equipment used enabled to get only two velocity components, the measurements were performed twice: the third velocity component was obtained through 90° rotation of the test rig between the two sets of measurements. The PDPA measurements focused on the region close to the origin of the jet, the seeding density being too low elsewhere. Two main planes were explored, located 30 mm and 60 mm from the point of emission and oriented normally to the main axis of the jet, as shown in Fig. 2. Additional data points were also taken through the vertical and horizontal planes of symmetry of the jet.

2.2. Gas phase measurements

The particle image velocimetry (PIV) technique was used to characterize the motion of the gas phase in the test rig. Illumination was realized through a frequency doubled Nd:Yag laser emitting 10 ns duration length pulses in 532 nm wavelength. Images were taken by a 12-bit, 1324 × 1024 pixels CCD HiSense MKII camera. Both single phase (i.e., without jet of solid particles) and two-phase measurements were carried out. 5 μm dolomite particles were used for seeding.

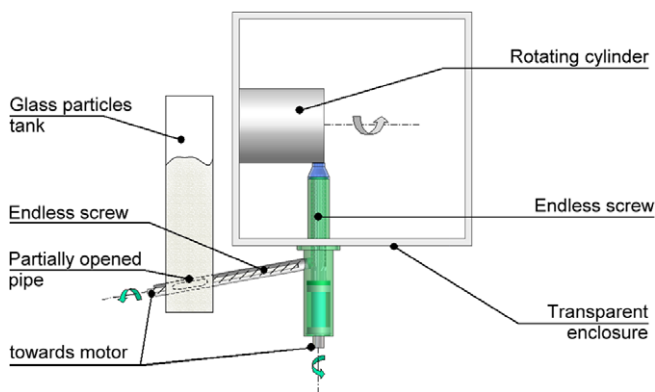


Fig. 1. Test rig and feeding system overview.

Table 1
Summary of test conditions and particle properties.

Cylinder rotation speed (rpm)	Cylinder peripheral speed (ms^{-1})	Particle mass flow rate (g s^{-1})	Particle average velocity from injection (% R)	Particle size distribution	Rosin–Rammler median diameter (μm)	Rosin–Rammler spread parameter
500	3.41	$1.5 \pm 6\%$	80.1%	100–200 μm	158.5	7.98
1000	6.83	$1.5 \pm 6\%$	81.4%	100–200 μm	158.5	7.98
1000	6.83	$0.955 \pm 6\%$	68%	50–150 μm	104.5	5.98
1000	6.83	0	–	–	–	–
500	3.41	0	–	–	–	–

Download English Version:

<https://daneshyari.com/en/article/667475>

Download Persian Version:

<https://daneshyari.com/article/667475>

[Daneshyari.com](https://daneshyari.com)